

3  
4 **Mitochondrial respiratory states and rates**

5  
6 Gnaiger Erich et al (MitoEAGLE Task Group)\*

7  
8 Corresponding author: Erich Gnaiger

9 *Chair COST Action CA15203 MitoEAGLE – <http://www.mitoeagle.org>*

10 *Department of Visceral, Transplant and Thoracic Surgery, D. Swarovski Research Laboratory,*

11 *Medical University of Innsbruck, Innrain 66/4, A-6020 Innsbruck, Austria*

12 *Email: mitoeagle@i-med.ac.at; Tel: +43 512 566796, Fax: +43 512 566796 20*

13  
14 Running title: Mitochondrial states and rates

15  
16 **As the knowledge base and importance of mitochondrial physiology to evolution, health, and**  
17 **disease expands, the necessity for harmonizing the terminology concerning mitochondrial**  
18 **respiratory states and rates has become increasingly apparent. The chemiosmotic theory**  
19 **establishes the mechanism of energy transformation during the process of oxidative**  
20 **phosphorylation (OXPHOS), providing the theoretical foundation of mitochondrial physiology**  
21 **and bioenergetics. We follow guidelines of the International Union of Pure and Applied Chemistry**  
22 **(IUPAC) on terminology, extended by considerations of mitochondrial respiratory control,**  
23 **metabolic flows and fluxes. The OXPHOS-capacity is respiration measured at kinetically-**  
24 **saturating concentrations of adenosine diphosphate, inorganic phosphate, and oxidizable**  
25 **substrates. The oxidative electron transfer-capacity reveals a possible limitation of OXPHOS-**  
26 **capacity mediated by the phosphorylation-pathway and is measured as noncoupled respiration at**  
27 **optimum concentrations of external uncouplers. Intrinsically uncoupled oxygen consumption**  
28 **compensates for ion leaks, particularly the proton leak. This LEAK-respiration is studied in the**  
29 **absence of ADP or by inhibition of the phosphorylation-pathway. Uniform standards for**  
30 **evaluation of respiratory states and rates will ultimately contribute to reproducibility between**  
31 **laboratories and thus support the development of databases of mitochondrial respiratory function**  
32 **in species, tissues, and cell types. Clarity of concept and consistency of nomenclature facilitate**  
33 **effective transdisciplinary communication, education, and ultimately further discovery.**

34  
35 *Keywords:* Mitochondrial respiratory control, coupling control; mitochondrial preparations;  
36 protonmotive force: *pmF*; uncoupling; oxidative phosphorylation: OXPHOS; electron transfer: ET;  
37 electron transfer system: ETS; proton leak, ion leak and slip compensatory state: LEAK; residual oxygen  
38 consumption: ROX; State 2; State 3; State 4; normalization; flow; flux; oxygen: O<sub>2</sub>; nicotinamide  
39 adenine dinucleotide: NADH

40  
41 **Harmonization of nomenclature**

42  
43 Mitochondria are essential cellular, membrane-enclosed organelles that perform a wide range of  
44 functions critical for cell viability. Their best-known function is to synthesize adenosine triphosphate  
45 (ATP) *via* oxidative phosphorylation (OXPHOS), however, they also have essential functions related to  
46 cellular metabolism and cell-signalling. This importance has led to an increasing body of research  
47 devoted to better understanding mitochondrial respiratory function. However, the dissemination of  
48 fundamental knowledge and implementation of novel discoveries require communication with a  
49 commonly understood terminology. Reproducibility of experimental procedures also depends on  
50 strictly-defined conditions and harmonization of shared research protocols. Unfortunately, a consensus  
51 on nomenclature and conceptual coherence is currently missing in the expanding field of mitochondrial  
52 physiology and bioenergetics. The use of vague, ambiguous, or inconsistent terminology likely  
53 contributes to confusion, miscommunication, and the conversion of valuable signals to wasteful noise.

54 Thus, complementary to quality control a conceptual framework is required to standardise and  
55 harmonise terminology and methodology.

56 To fill this communication gap, this perspective aims to harmonize nomenclature and addresses  
57 the terminology on coupling states and fluxes through metabolic pathways of aerobic energy  
58 transformation in mitochondrial (mt) preparations. In an attempt to establish a transdisciplinary  
59 nomenclature, we strive to incorporate a concept-driven terminology of bioenergetics with explicit,  
60 easily recognizable terms and symbols that define mitochondrial respiratory states and rates. The  
61 consistent use of terms and symbols will facilitate transdisciplinary communication for quantitative  
62 modelling and data repositories on bioenergetics and mitochondrial physiology<sup>1-3</sup>.

## 64 Coupling in mitochondrial respiration

65  
66 **Respiration and fermentation.** Aerobic respiration is the O<sub>2</sub> flux in (1) OXPHOS with catabolic  
67 reactions leading to O<sub>2</sub> consumption coupled to phosphorylation of ADP to ATP, plus (2) O<sub>2</sub> consuming  
68 reactions apart from OXPHOS. Coupling of electron transfer (ET) to ADP→ATP conversion is mediated  
69 by vectorial translocation of protons across the mitochondrial inner membrane (mtIM). Proton pumps  
70 generate, or utilize the electrochemical protonmotive force, *pmF* (Fig. 1). The *pmF* is the sum of two  
71 partial forces, the electric force (electric potential difference across the mtIM) and chemical force  
72 (proton chemical potential difference, related to  $\Delta\text{pH}$ )<sup>4,5</sup>. Cell respiration is thus distinguished from  
73 fermentation: (1) Compartmental coupling in vectorial OXPHOS contrasts to substrate-level  
74 phosphorylation in fermentation without requirement for O<sub>2</sub><sup>4,5</sup>. (2) Redox balance is maintained in  
75 aerobic respiration by O<sub>2</sub> as the electron acceptor supplied externally, whereas fermentation is  
76 characterized by internal electron acceptors formed in intermediary metabolism (Fig. 1a).

77  
78 **Respiratory states and respiratory capacity.** Cell membranes include organellar membranes and the  
79 plasma membrane, which separates the intracellular milieu from the extracellular environment (Fig. 1a).  
80 The plasma membrane consists of a lipid bilayer with embedded proteins and attached organic  
81 molecules that collectively control the selective permeability of ions, organic molecules and particles,  
82 limiting the passage of many water-soluble mitochondrial substrates and inorganic ions. Such limitations  
83 are overcome in mitochondrial preparations: plasma membranes are removed or selectively  
84 permeabilized, while mitochondrial structural and functional integrity is maintained<sup>6</sup>. In mt-  
85 preparations, extramitochondrial concentrations of oxidizable 'fuel' substrates, ADP, ATP, inorganic  
86 phosphate (P<sub>i</sub>), and cations including H<sup>+</sup> can be controlled to determine mitochondrial respiratory  
87 function under a set of conditions defined as coupling control states (Tab. 1). In substrate-uncoupler-  
88 inhibitor titration protocols, substrate combinations and specific inhibitors of ET-pathway enzymes are  
89 used to obtain defined pathway control states<sup>7,8</sup> (Fig. 1b). Pathway and coupling control states are  
90 complementary, since mt-preparations depend on (1) an exogenous supply of pathway-specific fuel  
91 substrates and O<sub>2</sub>, and (2) exogenous control of phosphorylation<sup>9</sup>.

92 Reference respiratory states are established with kinetically-saturating substrate concentrations  
93 for analysis of mitochondrial respiratory capacities. These delineate — comparable to channel capacity  
94 in information theory<sup>10</sup> — the upper limit of O<sub>2</sub> consumption rates. Intracellular conditions in living  
95 cells may deviate from these experimental states. Further information is obtained in kinetic studies of  
96 flux as a function of fuel substrate concentration, [ADP], or [O<sub>2</sub>] in the range between kinetically-  
97 saturating concentrations and anoxia<sup>11</sup>.

98  
99 **Phosphorylation.** The term phosphorylation is used generally in many contexts, *e.g.*, protein  
100 phosphorylation. Phosphorylation in the context of OXPHOS is defined as phosphorylation of ADP by  
101 P<sub>i</sub> to form ATP, coupled to oxidative electron transfer (Fig. 1c,d). The ET- and phosphorylation-  
102 pathways comprise coupled components of the OXPHOS-system. P/O is the ratio of P<sub>i</sub> to atomic oxygen  
103 consumed<sup>9</sup>. The symbol, P<sub>»</sub>, is introduced here as more discriminating and specific than P (Fig. 1c). The  
104 symbol P<sub>»</sub> indicates the endergonic (uphill) direction ADP→ATP, and likewise P<sub>«</sub> the corresponding  
105 exergonic (downhill) hydrolysis ATP→ADP (Fig. 2). *J*<sub>P<sub>»</sub> and *J*<sub>P<sub>«</sub> are the corresponding fluxes of ADP  
106 phosphorylation and ATP hydrolysis, respectively. P<sub>»</sub> refers to phosphorylation driven by proton  
107 translocation (Fig. 1d)<sup>12</sup>, but may also involve substrate-level phosphorylation in the mitochondrial  
108 matrix (succinyl-CoA ligase, monofunctional C1-tetrahydrofolate synthase), cytosol (phosphoglycerate  
109 kinase and pyruvate kinase), or both (phosphoenolpyruvate carboxykinase isoforms 1 and 2). Kinase</sub></sub>

110 cycles are involved in intracellular energy transfer and signal transduction for regulation of energy  
111 flux<sup>13</sup>.

112

## 113 **Respiratory coupling control states: concept and nomenclature**

114

115 **Concept-driven terminology.** Respiratory control refers to the ability of mitochondria to adjust O<sub>2</sub> flux  
116 in response to external control signals by engaging various mechanisms of control and regulation<sup>14</sup>.  
117 Respiratory control is monitored in mt-preparations under conditions defined as ‘respiratory states’,  
118 preferentially under near-physiological conditions of temperature, pH, and medium ionic composition.  
119 When phosphorylation of ADP to ATP is stimulated or depressed, an increase or decrease is observed  
120 in electron transfer. This is measured as O<sub>2</sub> flux in respiratory coupling states of intact mitochondria  
121 (‘controlled states’ in the classical terminology of bioenergetics). Alternatively, the coupling of electron  
122 transfer with phosphorylation is diminished by uncouplers, which eliminates control by P<sub>»</sub> and may  
123 increase respiratory rate (noncoupled or ‘uncontrolled state’; **Tab. 1**).

124 Coupling efficiency is diminished by both intrinsic and extrinsic uncoupling. Uncoupling of  
125 mitochondrial respiration is a general term comprising diverse mechanisms. Differences of terms —  
126 uncoupled *vs.* noncoupled — are easily overlooked, although they relate to different meanings of  
127 uncoupling (**Tab. 2**).

128 To extend the classical nomenclature on mitochondrial states (State 1 to 5)<sup>15</sup> by a concept-driven  
129 terminology that explicitly incorporates information on the meaning of respiratory states, the  
130 terminology must be general, and not restricted to any particular experimental protocol or type of  
131 mitochondrial preparation<sup>16</sup>. Standard respiratory coupling states are obtained while maintaining a  
132 defined ET-pathway state with constant fuel substrates and inhibitors of specific branches of the ET-  
133 pathway. The focus of concept-driven nomenclature is primarily the theoretical *why*, along with  
134 clarification of the experimental *how*<sup>17</sup>.

135 In the three coupling states — LEAK, OXPHOS, and ET — the corresponding respiratory rates  
136 are abbreviated as *L*, *P*, and *E*, respectively (**Fig. 2a**). The *pmF* is *maximum* in the LEAK-state of coupled  
137 mitochondria, driven by LEAK-respiration at a minimum back-flux of cations to the matrix  
138 compartment, *high* in the OXPHOS-state when it drives phosphorylation, and *low* in the ET-state when  
139 uncouplers short-circuit the proton cycle (**Tab. 1**).

140

141 **LEAK-state - Fig. 2b.** The LEAK-state is the state of mitochondrial respiration when O<sub>2</sub> flux mainly  
142 compensates for ion leaks in the absence of ATP synthesis at kinetically-saturating concentrations of O<sub>2</sub>  
143 and fuel substrates. Stimulation of phosphorylation is prevented by (1) absence of ADP and ATP; (2)  
144 maximum ATP/ADP ratio (State 4); or (3) inhibition of the phosphorylation-pathway with inhibitors of  
145 F<sub>1</sub>F<sub>0</sub>-ATPase (oligomycin; Omy) or adenine nucleotide translocase (carboxyatractyloside; **Tab. 1**). The  
146 chelator EGTA is added to mt-respiration media to bind free Ca<sup>2+</sup>, thus limiting cation cycling. LEAK-  
147 respiration is the intrinsically uncoupled O<sub>2</sub> consumption without addition of uncouplers. The LEAK-  
148 rate is a function of respiratory state, hence it depends on (1) the barrier function of the mtIM  
149 (‘leakiness’), (2) the electrochemical potential differences and concentration differences across the  
150 mtIM, and (3) the H<sup>+</sup>/O<sub>2</sub> ratio of the ET-pathway (**Fig. 1b**).

151 State 4 is a LEAK-state after depletion of ADP<sup>15</sup>. O<sub>2</sub> flux in State 4 overestimates LEAK-  
152 respiration if ATP hydrolysis activity recycles ATP to ADP,  $J_{P_{«}}$ , which stimulates respiration coupled  
153 to phosphorylation,  $J_{P_{»}} > 0$ . Inhibition of the phosphorylation-pathway by oligomycin ensures that  $J_{P_{»}} =$   
154 0 (State 4o; **Tab. 1**).

155

156 **OXPHOS-state - Fig. 2c.** At any given ET-pathway state, the OXPHOS-state establishes conditions to  
157 measure OXPHOS-capacity as a reference, at kinetically-saturating concentrations of O<sub>2</sub>, as well as fuel  
158 and phosphorylation substrates. Respiratory OXPHOS-capacities, *P*, are related to ADP-  
159 phosphorylation capacities by the ATP yield per O<sub>2</sub> (**Fig. 1c**).

160 The OXPHOS-state is compared with State 3, which is the state stimulated by addition of fuel  
161 substrates while the ADP concentration in the preceding State 2 (see below) is still ‘high’ and supports  
162 coupled energy transformation in isolated mitochondria in a closed respirometric chamber<sup>15</sup>. Repeated  
163 ADP titrations re-establish State 3. Starting at experimental O<sub>2</sub> concentrations of air-saturation (193 or  
164 238 μM O<sub>2</sub> at 37 °C or 25 °C and sea level at 1 atm or 101.32 kPa, and an O<sub>2</sub> solubility of respiration  
165 medium at 0.92 times that of pure water)<sup>18</sup>, the ADP concentrations must be low enough (typically 100

166 to 300  $\mu\text{M}$ ) to allow phosphorylation to ATP without  $\text{O}_2$  depletion during the transition to State 4. In  
 167 contrast, kinetically-saturating ADP concentrations are usually 10-fold higher than 'high ADP' (e.g., 2.5  
 168 mM) supporting OXPHOS capacity in isolated mitochondria<sup>11</sup>.

169  
 170 **Electron transfer-state - Fig. 2d.** The ET-state is defined as the *noncoupled* state with kinetically-  
 171 saturating concentrations of  $\text{O}_2$  and respiratory substrate, at the optimum concentration of exogenous  
 172 uncoupler for maximum  $\text{O}_2$  flux (ET-capacity). Uncouplers are weak lipid-soluble acids that function  
 173 as protonophores. These disrupt the barrier function of the mtIM and thus short-circuit the protonmotive  
 174 system, functioning like a clutch in a mechanical device. As a consequence of the nearly collapsed *pmF*,  
 175 the driving force is insufficient for phosphorylation and  $J_{\text{P}_s} = 0$ . The most frequently used uncouplers  
 176 are carbonyl cyanide *m*-chloro phenyl hydrazone (CCCP), carbonyl cyanide *p*-  
 177 trifluoromethoxyphenylhydrazone (FCCP), or dinitrophenol (DNP). Stepwise titration of uncouplers  
 178 stimulates respiration up to or above the level of  $\text{O}_2$  consumption rates in the OXPHOS-state; respiration  
 179 is inhibited, however, above optimum uncoupler concentrations<sup>5</sup>.

180 The abbreviation State 3u is occasionally used to indicate the state of respiration after titration of  
 181 an uncoupler, without sufficient emphasis on the fundamental difference between OXPHOS-capacity  
 182 (*well-coupled* with an endogenous uncoupled component) and ET-capacity (*noncoupled*; Fig. 2a).

183  
 184 **ROX-state versus anoxia.** The state of residual  $\text{O}_2$  consumption, ROX, is not a coupling state. The rate  
 185 of residual oxygen consumption, *Rox*, is defined as  $\text{O}_2$  consumption due to oxidative reactions measured  
 186 after inhibition of ET with antimycin A alone, or in combination with rotenone and malonic acid.  
 187 Cyanide and azide not only inhibit CIV, but also catalase and several peroxidases, whereas alternative  
 188 quinol oxidase is not inhibited (Fig. 1b). *Rox* represents a baseline to correct respiration: *Rox*-corrected  
 189 *L*, *P* and *E* are not only lower than total fluxes, but also change the flux control ratios *L/P* and *L/E*. *Rox*  
 190 is not necessarily equivalent to non-mitochondrial respiration. This is important when considering  $\text{O}_2$ -  
 191 consuming reactions in mitochondria that are not related to ET — such as  $\text{O}_2$  consumption in reactions  
 192 catalyzed by monoamine oxidases, monooxygenases (cytochrome P450 monooxygenases),  
 193 dioxygenases (trimethyllysine dioxygenase), and several hydroxylases.

194 In the nomenclature of Chance and Williams, State 2 is induced by titration of ADP before  
 195 addition of oxidizable substrates<sup>15,19</sup>. ADP stimulates respiration transiently on the basis of endogenous  
 196 fuel substrates resulting in phosphorylation of a small portion of the added ADP. State 2 is then a ROX  
 197 state at minimum respiratory activity after exhaustion of endogenous fuel substrates. State 5 '*may be*  
 198 *obtained by antimycin A treatment or by anaerobiosis*'<sup>15</sup>. These definitions give State 5 two different  
 199 meanings: ROX or anoxia.

200 Anoxia is induced after exhaustion of  $\text{O}_2$  in a closed respirometric chamber. Diffusion of  $\text{O}_2$  from  
 201 the surroundings into the aqueous solution is a confounding factor potentially preventing complete  
 202 anoxia<sup>11</sup>.

203

## 204 Rates and SI units

205

206 The term *rate* is not adequately defined to be useful for reporting data. A rate can be an extensive  
 207 quantity<sup>1</sup>, termed *flow*, *I*, when expressed (1) per chamber (instrumental system), or (2) per countable  
 208 object (number of cells, organisms,  $N_x$ ). Alternatively, a rate is a size-specific quantity<sup>2</sup>, termed *flux*, *J*,  
 209 when expressed (3) per volume of the chamber, *V*, or (4) per volume of the sample,  $V_x$ , or mass,  $m_x$  (Fig.  
 210 3).

211 Different units are used to report the  $\text{O}_2$  consumption rate, OCR. SI units provide a common  
 212 reference with appropriately chosen SI prefixes<sup>1</sup>. Although volume is expressed as  $\text{m}^3$  using the SI base  
 213 unit, the liter [ $\text{dm}^3$ ] is a conventional unit of volume for concentration and is used for most solution  
 214 kinetics. Constants for conversion to SI units are summarized in Tab. 3a.

215

## 216 Normalization of rate per system

217

218 **Flow: per chamber.** The instrumental system (chamber) is part of the measurement instrument,  
 219 separated from the environment by a closed or open system boundary. Analyses are restricted to intra-

220 experimental comparison of relative differences, when reporting  $O_2$  flows per respiratory chamber,  $I_{O_2}$   
 221  $[\text{mol}\cdot\text{s}^{-1}]$  (Fig. 3).

222

223 **Flux: per chamber volume.** System volume-specific  $O_2$  flux,  $J_{V,O_2}$  (per liquid  $V$  of the instrumental  
 224 chamber  $[\text{L}=\text{dm}^3]$ ), is of methodological interest in relation to the instrumental limit of detection.  $J_{V,O_2}$   
 225 increases in proportion to sample concentration in the chamber.  $J_{V,O_2}$  should be independent of the  
 226 chamber volume at constant sample concentration. There are practical limitations to increasing the  
 227 sample concentration in the chamber, when one is concerned about crowding effects and instrumental  
 228 time resolution.

229

## 230 Normalization of rate per sample

231

232 **Flow: per object.** A sample,  $X$ , may contain countable, non-divisible ('in-dividual') objects with a  
 233 variable number of objects,  $N_X$ . The number concentration of  $X$  is  $C_{NX}$ . Accordingly, the experimental  
 234 number concentration of cells,  $C_{Nce} = N_{ce}\cdot V^{-1}$ , is the number of cells,  $N_{ce}$  [x], per chamber volume,  $V$  [L].  
 235 Volume-specific  $O_2$  flux,  $J_{V,O_2}$   $[\text{mol}\cdot\text{s}^{-1}\cdot\text{L}^{-1}]$  divided by  $C_{NX}$   $[\text{x}\cdot\text{L}^{-1}]$  yields the oxygen flow per cell,  $I_{O_2/Nce}$   
 236  $[\text{mol}\cdot\text{s}^{-1}\cdot\text{x}^{-1}]$ . Here we write the dimensionless non-SI unit [x] explicitly, to distinguish the unit for flow  
 237 per object,  $I_{O_2/NX}$   $[\text{mol}\cdot\text{s}^{-1}\cdot\text{x}^{-1}]$ , from flow per chamber,  $I_{O_2}$   $[\text{mol}\cdot\text{s}^{-1}]$ . For convenience,  $O_2$  flow is  
 238 expressed in units of attomole ( $10^{-18}$  mol) of  $O_2$  consumed per second per cell  $[\text{amol}\cdot\text{s}^{-1}\cdot\text{ce}^{-1}]$ <sup>20</sup>,  
 239 numerically equivalent to  $[\text{pmol}\cdot\text{s}^{-1}\cdot(10^6\text{ ce})^{-1}]$ . At an  $O_2$  flow of  $100\text{ amol}\cdot\text{s}^{-1}\cdot\text{ce}^{-1}$  and a cell concentration  
 240 of  $10^9\text{ ce}\cdot\text{L}^{-1}$  ( $=10^6\text{ ce}\cdot\text{mL}^{-1}$ ),  $J_{V,O_2}$  is  $100\text{ nmol}\cdot\text{s}^{-1}\cdot\text{L}^{-1}$  ( $=100\text{ pmol}\cdot\text{s}^{-1}\cdot\text{mL}^{-1}$ ; Tab. 3b).

241

242 **Size-specific flux: per sample size.** Several sample types are not quantifiable numerically, *e.g.*, tissue  
 243 homogenate, in which case a sample-specific oxygen flow cannot be expressed discretely. Mass-specific  
 244 flux,  $J_{O_2/mX}$   $[\text{mol}\cdot\text{s}^{-1}\cdot\text{kg}^{-1}]$ , expresses respiration normalized per mass of the sample. Mass-specific oxygen  
 245 flux integrates the quality and density of mitochondria, and thus provides the appropriate normalization  
 246 for evaluation of tissue performance. When studying isolated mitochondria and homogenized or  
 247 permeabilized tissues and cells,  $J_{O_2/mX}$  should be independent of the mass-concentration of the subsample  
 248 obtained from the same tissue or cell culture.  $I_{O_2/Nce}$  can be directly compared only between cells of  
 249 identical size. To take into account differences in cell size, normalization is required to obtain cell size-  
 250 specific flux,  $J_{O_2/mce}$  or  $J_{O_2/Vce}$ <sup>21</sup> (Fig. 3).

251

252 **Marker-specific flux: per mitochondrial content.** To evaluate differences in mitochondrial respiration  
 253 independent of mitochondrial density, flux is normalized for structural or functional mt-elementary  
 254 markers, *mtE*, expressed in marker-specific mt-elementary units [mtEU] (Fig. 3). For example, citrate  
 255 synthase (CS) activity is a frequently applied functional *mtE* expressed in international units, IU  
 256  $[\mu\text{mol}\cdot\text{min}^{-1}]$  (1 IU of CS forms 1  $\mu\text{mol}$  of citrate per min; although the SI unit  $[\text{nmol}\cdot\text{s}^{-1}]$  would be  
 257 preferable). Then the mtEU is taken as  $[\mu\text{mol}\cdot\text{min}^{-1}]$  or  $[\text{nmol}\cdot\text{s}^{-1}]$ . Volume-specific oxygen flux,  $J_{V,O_2}$   
 258  $[\text{pmol}\cdot\text{s}^{-1}\cdot\text{mL}^{-1}]$ , is divided by CS activity expressed per chamber volume  $[\text{mtEU}\cdot\text{mL}^{-1}]$ , to obtain marker-  
 259 specific respiratory flux,  $J_{O_2/mtE}$   $[\text{pmol}\cdot\text{s}^{-1}\cdot\text{mtEU}^{-1}]$ . Alternatively,  $J_{O_2/mtE}$  is calculated from tissue mass-  
 260 specific flux of permeabilized muscle fibers,  $J_{O_2/m}$   $[\text{pmol}\text{ O}_2\cdot\text{s}^{-1}\cdot\text{mg}^{-1}]$ , divided by tissue mass-specific  
 261 CS activity  $[\text{mtEU}\cdot\text{mg}^{-1}]$ .  $J_{O_2/mtE}$  is independent of mitochondrial density. If the respirometric and  
 262 enzymatic assays are performed at an identical temperature, OXPHOS- or ET-capacity can be compared  
 263 with the capacity of CS as a regulatory enzyme in the tricarboxylic acid (TCA) cycle, which is of interest  
 264 in the context of metabolic flux control.

265 One cannot assume that quantitative changes in various markers — such as CS activity, other  
 266 mitochondrial enzyme activities or protein content — occur in parallel with one another<sup>22</sup>. It should be  
 267 established that the marker chosen is not selectively altered by the compared trait or treatment. In  
 268 conclusion, the normalization must reflect the question under investigation. On the other hand, the goal  
 269 of combining results across projects and institutions requires standardization of normalization for entry  
 270 into a databank.

271

272 Comparable to the concept of the respiratory acceptor control ratio,  $RCR = \text{State 3}/\text{State 4}$  (ref. <sup>9</sup>),  
 273 the most readily applied normalization is that of flux control ratios and flux control factors<sup>8,16</sup>. Then,  
 274 instead of a specific mt-enzyme activity, the respiratory activity in a reference state serves as the *mtE*,  
 yielding a dimensionless ratio of two fluxes measured consecutively in the same respirometric titration

275 protocol. Selection of the state of maximum flux in a protocol as the reference state — *e.g.*, ET-state in  
 276 *L/E* and *P/E* flux control ratios<sup>16</sup> — has the advantages of: (1) elimination of experimental variability in  
 277 additional measurements, such as determination of enzyme activity or tissue mass; (2) statistically  
 278 validated linearization of the response in the range of 0 to 1; and (3) consideration of maximum flux for  
 279 integrating a large number of metabolic steps in the OXPHOS- or ET-pathways. This reduces the risk  
 280 of selecting a functional marker that is specifically altered by the treatment or pathology, yet increases  
 281 the chance that the highly integrative pathway is affected, *e.g.*, the OXPHOS- rather than ET-pathway  
 282 in case of an enzymatic defect in the phosphorylation-pathway. In this case, additional information can  
 283 be obtained by reporting flux control ratios based on a reference state that indicates stable tissue mass-  
 284 specific flux.

## 286 Conclusions

287  
 288 Clarity of concepts on mitochondrial respiratory control can serve as a gateway to better diagnose  
 289 mitochondrial respiratory adaptations and defects linked to genetic variation, age-related health risks,  
 290 sex-specific mitochondrial performance, lifestyle with its effects on degenerative diseases, and thermal  
 291 and chemical environment. The challenges of measuring mitochondrial respiratory flux are matched by  
 292 those of normalization: We distinguish between (1) the instrumental *system* or *chamber* with volume *V*  
 293 and mass *m* defined by the system boundaries, and (2) the *sample* or *objects* with volume *V<sub>X</sub>* and mass  
 294 *m<sub>X</sub>* that are enclosed in the instrumental chamber. Metabolic O<sub>2</sub> *flow* per countable object increases as  
 295 the size of the object is increased. This confounding factor is eliminated by expressing respiration as  
 296 mass-specific or cell volume-specific O<sub>2</sub> *flux*. The present recommendations on coupling control states  
 297 and respiratory rates are focused on studies using mitochondrial preparations. Terms and symbols are  
 298 summarized in [Tab. 4](#). These need to be complemented by considerations on pathway control of  
 299 mitochondrial respiration<sup>7,8,23</sup>, respiratory states and rates in living cells, respiratory flux control ratios,  
 300 and harmonization of experimental procedures. The present perspective is extended in a more detailed  
 301 overview on mitochondrial physiology<sup>24</sup>.

## 303 References

- 304
- 305 1. Cohen, E. R. et al. *IUPAC Green Book, 3rd Edition, 2nd Printing, IUPAC & RSC Publishing, Cambridge*  
 306 (2008).
- 307 2. Gnaiger, E. *Pure Appl Chem* **65**, 1983-2002 (1993).
- 308 3. Beard, D. A. *PLoS Comput Biol* **1**, e36 (2005).
- 309 4. Mitchell, P. *Nature* **191**, 144-148 (1961).
- 310 5. Mitchell, P. *Biochim Biophys Acta Bioenergetics* **1807**, 1507-1538 (2011).
- 311 6. Schmitt, S. et al. *Anal Biochem* **443**, 66-74 (2013).
- 312 7. Doerrier, C. et al. *Methods Mol Biol* **1782**, 31-70 (2018).
- 313 8. §Gnaiger, E. *Bioenerg Commun* **2020.2**, doi:10.26124/bec:2020-0002.v1 (2020).
- 314 9. Chance, B. & Williams, G. R. *J Biol Chem* **217**, 383-393 (1955).
- 315 10. Schneider, T. D. *IEEE Eng Med Biol Mag* **25**, 30-33 (2006).
- 316 11. Gnaiger, E. *Respir Physiol* **128**, 277-297 (2001).
- 317 12. Watt, I. N. et al. *Proc Natl Acad Sci U S A* **107**, 16823-16827 (2010).
- 318 13. Németh, B. et al. *FASEB J* **30**, 286-300 (2016).
- 319 14. Fell, D. *Understanding the control of metabolism. Portland Press* (1997).
- 320 15. Chance, B. & Williams, G. R. *J Biol Chem* **217**, 409-427 (1955).
- 321 16. Gnaiger, E. *Int J Biochem Cell Biol* **41**, 1837-1845 (2009).
- 322 17. Miller, G. A. *The science of words. Scientific American Library New York* (1991).
- 323 18. Forstner, H. & Gnaiger, E. In: *Polarographic Oxygen Sensors. Aquatic and Physiological Applications.*  
 324 *Gnaiger, E. & Forstner, H. (eds), Springer, Berlin, Heidelberg, New York, 321-333* (1983).
- 325 19. Chance, B. & Williams, G. R. *Adv Enzymol Relat Subj Biochem* **17**, 65-134 (1956).
- 326 20. Wagner, B. A., Venkataraman, S. & Buettner, G. R. *Free Radic Biol Med* **51**, 700-712 (2011).
- 327 21. Renner, K. et al. *Biochim Biophys Acta* **1642**, 115-123 (2003).
- 328 22. Drahotka, Z. et al. *Physiol Res* **53**, 119-122 (2004).
- 329 23. Schöpf, B. et al. *Nat Commun* **11**, 1487 (2020).
- 330 24. §Gnaiger, E. et al. *Bioenerg Commun* **2020.1**, doi:10.26124/bec:2020-0001.v1 (2020).
- 331 25. Canton, M. et al. *Biochem J* **310**, 477-481 (1995).
- 332 26. Mohr, P.J. & Phillips, W.D. *Metrologia* **52**, 40-47 (2015).

- 333 27. Rich, P. R. *Encyclopedia Biol Chem* **1**, 467-472 (2013).  
334 28. Lemieux, H., Blier, P. U. & Gnaiger, E. *Sci Rep* **7**, 2840 (2017).

335  
336  To be released with DOI until acceptance by *Nat Metab*

337 *At present:*

- 338 8. Gnaiger, E. *Mitochondr Physiol Network 19.12. Oroboros MiPNet Publications, Innsbruck* (2014).  
339 24. Gnaiger, E. et al. *MitoFit Preprint Arch* doi:10.26124/mitofit:190001.v6 (2019).

340  
341 **\*Authors (MitoEAGLE Task Group):** Gnaiger Erich, Aasander Frostner Eleonor, Abdul Karim  
342 Norwahidah, Abdel-Rahman Engy Ali, Abumrad Nada A, Acuna-Castroviejo Dario, Adiele Reginald  
343 C, Ahn Bumsoo, Alencar Mayke Bezerra, Ali Sameh S, Almeida Angeles, Alton Lesley, Alves Marco  
344 G, Amati Francesca, Amoedo Nivea Dias, Amorim Ricardo, Anderson Ethan J, Andreadou Ioanna,  
345 Antunes Diana, Arago Marc, Aral Cenk, Arandarcikaite Odeta, Arias-Reyes Christian, Armand Anne-  
346 Sophie, Arnould Thierry, Avram Vlad F, Axelrod Christopher L, Bailey Damian M, Bairam Aida,  
347 Bajpeyi Sudip, Bajzikova Martina, Bakker Barbara M, Banni Aml, Bardal Tora, Barlow J, Bastos  
348 Sant'Anna Silva Ana Carolina, Batterson Philip M, Battino Maurizio, Bazil Jason N, Beard Daniel A,  
349 Bednarczyk Piotr, Beleza Jorge, Bello Fiona, Ben-Shachar Dorit, Bento Guida Jose Freitas, Bergdahl  
350 Andreas, Berge Rolf K, Bergmeister Lisa, Bernardi Paolo, Berridge Michael V, Bettinazzi Stefano,  
351 Bishop David J, Blier Pierre U, Blindheim Dan Filip, Boardman Neoma T, Boetker Hans Erik, Borchard  
352 Sabine, Boros Mihaly, Boersheim Elisabet, Borrás Consuelo, Borutaite Vilma, Botella Javier, Bouillaud  
353 Frederic, Bouitbir Jamal, Boushel Robert C, Bovard Josh, Bravo-Sagua Roberto, Breton Sophie, Brown  
354 David A, Brown Guy C, Brown Robert Andrew, Brozinick Joseph T, Buettner Garry R, Burtscher  
355 Johannes, Bustos Matilde, Calabria Elisa, Calbet Jose AL, Calzia Enrico, Cannon Daniel T, Cano  
356 Sanchez Maria Consolacion, Canto Alvarez Carles, Cardinale Daniele A, Cardoso Luiza HD, Carvalho  
357 Eugenia, Casado Pinna Marta, Cassar Samantha, Castelo Rueda Maria Paulina, Castilho Roger F,  
358 Cavalcanti-de-Albuquerque Joao Paulo, Cecatto Cristiane, Celen Murat C, Cervinkova Zuzana, Chabi  
359 Beatrice, Chakrabarti Lisa, Chakrabarti Sasanka, Chaurasia Bhagirath, Chen Quan, Chicco Adam J,  
360 Chinopoulos Christos, Chowdhury Subir Kumar, Cizmarova Beata, Clementi Emilio, Coen Paul M,  
361 Cohen Bruce H, Coker Robert H, Collin-Chenot Anne, Coughlan Melinda T, Coxito Pedro, Crisostomo  
362 Luis, Crispim Marcell, Crossland Hannah, Dahdah Norma Ramon, Dalgaard Louise T, Dambrova  
363 Maija, Danhelovska Tereza, Darveau Charles-A, Darwin Paula M, Das Anibh Martin, Dash Ranjan K,  
364 Davidova Eliska, Davis Michael S, Dayanidhi Sudarshan, De Bem Andreza Fabro, De Goede Paul, De  
365 Palma Clara, De Pinto Vito, Dela Flemming, Dembinska-Kiec Aldona, Detraux Damian, Devaux Yvan,  
366 Di Marcello Marco, Di Paola Floriana Jessica, Dias Candida, Dias Tania R, Diederich Marc, Distefano  
367 Giovanna, Djafarzadeh Siamak, Doermann Niklas, Doerrier Carolina, Dong Lan-Feng, Donnelly Chris,  
368 Drahota Zdenek, Duarte Filipe Valente, Dubouchaud Herve, Duchon Michael R, Dumas Jean-Francois,  
369 Durham William J, Dymkowska Dorota, Dyrstad Sissel E, Dyson Alex, Dzialowski Edward M, Eaton  
370 Simon, Ehinger Johannes K, Elmer Eskil, Endlicher Rene, Engin Ayse Basak, Escames Germaine,  
371 Evinova Andrea, Ezrova Zuzana, Falk Marni J, Fell David A, Ferdinandy Peter, Ferko Miroslav,  
372 Fernandez-Ortiz Marisol, Fernandez-Vizarra Erika, Ferreira Julio Cesar B, Ferreira Rita Maria P, Ferri  
373 Alessandra, Fessel Joshua Patrick, Festuccia William T, Filipovska Aleksandra, Fisar Zdenek, Fischer  
374 Christine, Fischer Michael J, Fisher Gordon, Fisher Joshua J, Fontanesi Flavia, Forbes-Hernandez  
375 Tamara Y, Ford Ellen, Fornaro Mara, Fuertes Agudo Marina, Fulton Montana, Galina Antonio, Galkin  
376 Alexander, Gallee Leon, Galli Gina L J, Gama Perez Pau, Gan Zhenji, Ganetzky Rebecca, Gao Yun,  
377 Garcia Geovana S, Garcia-Rivas Gerardo, Garcia-Roves Pablo Miguel, Garcia-Souza Luiz F, Garlid  
378 Keith D, Garrabou Gloria, Garten Antje, Gastaldelli Amalia, Gayen Jiaur, Genders Amanda J, Genova  
379 Maria Luisa, Giampieri Francesca, Giovarelli Matteo, Glatz Jan FC, Goikoetxea Usandizaga Naroa,  
380 Goncalo Teixeira da Silva Rui, Goncalves Debora Farina, Gonzalez-Armenta Jenny L, Gonzalez-  
381 Franquesa Alba, Gonzalez-Freire Marta, Gonzalo Hugo, Goodpaster Bret H, Gorr Thomas A, Gourlay  
382 Campbell W, Grams Bente, Granata Cesare, Grefte Sander, Grilo Luis, Guarch Meritxell Espino,  
383 Gueguen Naig, Gumeni Sentiljana, Haas Clarissa, Haavik Jan, Hachmo Yafit, Haendeler Judith, Haider  
384 Markus, Hajrulahovic Anesa, Hamann Andrea, Han Jin, Han Woo Hyun, Hancock Chad R, Hand Steven  
385 C, Handl Jiri, Hansikova Hana, Hardee Justin P, Hargreaves Iain P, Harper Mary-Ellen, Harrison David  
386 K, Hassan Hazirah, Hatokova Zuzana, Hausenloy Derek J, Heales Simon JR, Hecker Matthias, Heiestad  
387 Christina, Hellgren Kim T, Henrique Alexandrino, Hepple Russell T, Hernansanz-Agustin Pablo,  
388 Hewakapuge Sudinna, Hickey Anthony J, Ho Dieu Hien, Hoehn Kyle L, Hoel Fredrik, Holland Olivia  
389 J, Holloway Graham P, Holzner Lorenz, Hoppel Charles L, Hoppel Florian, Hoppeler Hans, Houstek

390 Josef, Huete-Ortega Maria, Hyrossova Petra, Iglesias-Gonzalez Javier, Irving Brian A, Isola Raffaella,  
391 Iyer Shilpa, Jackson Christopher Benjamin, Jadiya Pooja, Jana Prado Fabian, Jandeleit-Dahm Karin,  
392 Jang David H, Jang Young Charles, Janowska Joanna, Jansen Kirsten M, Jansen-Duerr Pidder, Jansone  
393 Baiba, Jarmuszkiewicz Wieslawa, Jaskiewicz Anna, Jaspers Richard T, Jedlicka Jan, Jerome Estaquier,  
394 Jespersen Nichlas Riise, Jha Rajan Kumar, Jones John G, Joseph Vincent, Jurczak Michael J, Jurk  
395 Diana, Jusic Amela, Kaambre Tuuli, Kaczor Jan Jacek, Kainulainen Heikki, Kampa Rafal Pawel,  
396 Kandel Sunil Mani, Kane Daniel A, Kapferer Werner, Kapnick Senta, Kappler Lisa, Karabatsiakis  
397 Alexander, Karavaeva Iuliia, Karkucinska-Wieckowska Agnieszka, Kaur Sarbjot, Keijer Jaap, Keller  
398 Markus A, Keppner Gloria, Khamoui Andy V, Kidere Dita, Kilbaugh Todd, Kim Hyoung Kyu, Kim  
399 Julian KS, Kimoloi Sammy, Klepinin Aleksandr, Klepinina Lyudmila, Klingenspor Martin, Klocker  
400 Helmut, Kolassa Iris, Komlodi Timea, Koopman Werner JH, Kopitar-Jerala Natasa, Kowaltowski Alicia  
401 J, Kozlov Andrey V, Krajcova Adela, Krako Jakovljevic Nina, Kristal Bruce S, Krycer James R, Kuang  
402 Jujiao, Kucera Otto, Kuka Janis, Kwak Hyo Bum, Kwast Kurt E, Kwon Oh Sung, Laasmaa Martin,  
403 Labieniec-Watala Magdalena, Lagarrigue Sylviane, Lai Nicola, Lalic Nebojsa M, Land John M, Lane  
404 Nick, Laner Verena, Lanza Ian R, Laouafa Sofien, Laranjinha Joao, Larsen Steen, Larsen Terje S,  
405 Lavery Gareth G, Lazou Antigone, Ledo Ana Margarida, Lee Hong Kyu, Leeuwenburgh Christiaan,  
406 Lehti Maarit, Lemieux Helene, Lenaz Giorgio, Lerfall Joergen, Li Pingan Andy, Li Puma Lance, Liang  
407 Liping, Liepins Edgars, Lin Chien-Te, Liu Jiankang, Lopez Garcia Luis Carlos, Lucchinetti Eliana, Ma  
408 Tao, Macedo Maria Paula, Machado Ivo F, Maciej Sarah, MacMillan-Crow Lee Ann, Magalhaes Jose,  
409 Magri Andrea, Majtnerova Pavlina, Makarova Elina, Makrecka-Kuka Marina, Malik Afshan N,  
410 Marcouiller Francois, Marechal Amandine, Markova Michaela, Markovic Ivanka, Martin Daniel S,  
411 Martins Ana Dias, Martins Joao D, Maseko Tumisang Edward, Maull Felicia, Mazat Jean-Pierre,  
412 McKenna Helen T, McKenzie Matthew, McMillan Duncan GG, McStay Gavin P, Mendham Amy,  
413 Menze Michael A, Mercer John R, Merz Tamara, Messina Angela, Meszaros Andras, Methner Axel,  
414 Michalak Slawomir, Mila Guasch Maria, Minuzzi Luciele M, Misirkic Marjanovic Maja, Moellering  
415 Douglas R, Moiso Nicoleta, Molina Anthony JA, Montaigne David, Moore Anthony L, Moore Christy,  
416 Moreau Kerrie, Moreira Bruno P, Moreno-Sanchez Rafael, Mracek Tomas, Muccini Anna Maria,  
417 Munro Daniel, Muntane Jordi, Muntean Danina M, Murray Andrew James, Musiol Eva, Nabben  
418 Miranda, Nair K Sreekumaran, Nehlin Jan O, Nemecek Michal, Nesci Salvatore, Neuffer P Darrell, Neuzil  
419 Jiri, Nevriere Remi, Newsom Sean A, Norman Jennifer, Nozickova Katerina, Nunes Sara, O'Brien  
420 Kristin, O'Brien Katie A, O'Gorman Donal, Olgar Yusuf, Oliveira Ben, Oliveira Jorge, Oliveira Marcus  
421 F, Oliveira Marcos Tulio, Oliveira Pedro Fontes, Oliveira Paulo J, Olsen Rolf Erik, Orynbayeva Zulfiya,  
422 Osiewacz Heinz D, Paez Hector, Pak Youngmi Kim, Pallotta Maria Luigia, Palmeira Carlos, Parajuli  
423 Nirmala, Passos Joao F, Passrigger Manuela, Patel Hemal H, Pavlova Nadia, Pavlovic Kasja, Pecina  
424 Petr, Pedersen Tina M, Perales Jose Carles, Pereira da Silva Grilo da Silva Filomena, Pereira Rita,  
425 Pereira Susana P, Perez Valencia Juan Alberto, Perks Kara L, Pesta Dominik, Petit Patrice X, Pettersen  
426 Nitschke Ina Katrine, Pichaud Nicolas, Pichler Irene, Piel Sarah, Pietka Terri A, Pinho Sonia A, Pino  
427 Maria F, Pirkmajer Sergej, Place Nicolas, Plangger Mario, Porter Craig, Porter Richard K, Pregoica  
428 Ines, Prigione Alessandro, Procaccio Vincent, Prochownik Edward V, Prola Alexandre, Pulinilkunnil  
429 Thomas, Puskarich Michael A, Puurand Marju, Radenkovic Filip, Ramzan Rabia, Rattan Suresh IS,  
430 Reano Simone, Reboredo-Rodriguez Patricia, Rees Bernard B, Renner-Sattler Kathrin, Rial Eduardo,  
431 Robinson Matthew M, Roden Michael, Rodrigues Ana Sofia, Rodriguez Enrique, Rodriguez-Enriquez  
432 Sara, Roesland Gro Vatne, Rohlena Jakub, Rolo Anabela Pinto, Ropelle Eduardo R, Roshanravan  
433 Baback, Rossignol Rodrigue, Rossiter Harry B, Rousar Tomas, Rubelj Ivica, Rybacka-Mossakowska  
434 Joanna, Saada Reisch Ann, Safaei Zahra, Salin Karine, Salvadego Desy, Sandi Carmen, Saner Nicholas,  
435 Santos Diana, Sanz Alberto, Sardao Vilma, Sarlak Saharnaz, Sazanov Leonid A, Scaife Paula, Scatena  
436 Roberto, Schartner Melanie, Scheibye-Knudsen Morten, Schilling Jan M, Schlattner Uwe, Schmitt  
437 Sabine, Schneider Gasser Edith Mariane, Schoenfeld Peter, Schots Pauke C, Schulz Rainer, Schwarzer  
438 Christoph, Scott Graham R, Selman Colin, Sendon Pamela Marie, Shabalina Irina G, Sharma Pushpa,  
439 Sharma Vipin, Shevchuk Igor, Shirazi Reza, Shiroma Jonathan G, Siewiera Karolina, Silber Ariel M,  
440 Silva Ana Maria, Sims Carrie A, Singer Dominique, Singh Brijesh Kumar, Skolik Robert A, Smenes  
441 Benedikte Therese, Smith James, Soares Felix Alexandre Antunes, Sobotka Ondrej, Sokolova Inna,  
442 Solesio Maria E, Soliz Jorge, Sommer Natascha, Sonkar Vijay K, Sova Marina, Sowton Alice P,  
443 Sparagna Genevieve C, Sparks Lauren M, Spinazzi Marco, Stankova Pavla, Starr Jonathan, Stary Creed,  
444 Stefan Eduard, Stelfa Gundega, Stepto Nigel K, Stevanovic Jelena, Stiban Johnny, Stier Antoine,  
445 Stocker Roland, Storder Julie, Sumbalova Zuzana, Suomalainen Anu, Suravajhala Prashanth, Svalbe



446 Baiba, Swerdlow Russell H, Swiniuch Daria, Szabo Ildiko, Szewczyk Adam, Szibor Marten, Tanaka  
447 Masashi, Tandler Bernard, Tarnopolsky Mark A, Tausan Daniel, Tavernarakis Nektarios, Teodoro Joao  
448 Soeiro, Tepp Kersti, Thakkar Himani, Thapa Maheshwor, Thyfault John P, Tomar Dhanendra, Ton  
449 Riccardo, Torp May-Kristin, Torres-Quesada Omar, Towheed Atif, Treberg Jason R, Tretter Laszlo,  
450 Trewin Adam J, Trifunovic Aleksandra, Trivigno Catherine, Tronstad Karl Johan, Trougakos Ioannis  
451 P, Truu Laura, Tuncay Erkan, Turan Belma, Tyrrell Daniel J, Urban Tomas, Urner Sofia, Valentine  
452 Joseph Marco, Van Bergen Nicole J, Van der Ende Miranda, Varricchio Frederick, Vaupel Peter, Vella  
453 Joanna, Vendelin Marko, Vercesi Anibal E, Verdaguer Ignasi Bofill, Vernerova Andrea, Victor Victor  
454 Manuel, Vieira Ligo Teixeira Camila, Vidimce Josif, Viel Christian, Vieyra Adalberto, Vilks Karlis,  
455 Villena Josep A, Vincent Vinnyfred, Vinogradov Andrey D, Viscomi Carlo, Vitorino Rui Miguel  
456 Pinheiro, Vlachaki Walker Julia, Vogt Sebastian, Volani Chiara, Volska Kristine, Votion Dominique-  
457 Marie, Vujacic-Mirski Ksenija, Wagner Brett A, Ward Marie Louise, Warnsmann Verena, Wasserman  
458 David H, Watala Cezary, Wei Yau-Huei, Weinberger Klaus M, Weissig Volkmar, White Sarah Haverty,  
459 Whitfield Jamie, Wickert Anika, Wieckowski Mariusz R, Wiesner Rudolf J, Williams Caroline M,  
460 Winwood-Smith Hugh, Wohlgemuth Stephanie E, Wohlwend Martin, Wolff Jonci Nikolai, Wrutniak-  
461 Cabello Chantal, Wuest Rob CI, Yokota Takashi, Zablocki Krzysztof, Zanon Alessandra, Zanou  
462 Nadege, Zaugg Kathrin, Zaugg Michael, Zdrzilova Lucie, Zhang Yong, Zhang Yizhu, Zikova Alena,  
463 Zischka Hans, Zorzano Antonio, Zujovic Tijana, Zvejniece Liga

Affiliations:

[https://www.bioenergetics-communications.org/index.php/BEC2020.1\\_doi10.26124bec2020-0001.v1](https://www.bioenergetics-communications.org/index.php/BEC2020.1_doi10.26124bec2020-0001.v1)

466

467

#### **Acknowledgements**

468

We thank Beno M for management assistance, and Rich PR for valuable discussions. This publication  
469 is based upon work from COST Action CA15203 MitoEAGLE, supported by COST (European  
470 Cooperation in Science and Technology), in cooperation with COST Actions CA16225 EU-  
471 CARDIOPROTECTION and CA17129 CardioRNA, and K-Regio project MitoFit funded by the  
472 Tyrolian Government.

473

474

#### **Author contributions**

475

This manuscript developed as an open invitation to scientists and students to join as coauthors in the  
476 bottom-up spirit of COST, based on a first draft written by the corresponding author, who integrated  
477 coauthor contributions in a sequence of Open Access versions. Coauthors contributed to the scope and  
478 quality of the manuscript, may have focused on a particular section, and are listed in alphabetical order.  
479 Coauthors confirm that they have read the final manuscript and agree to implement the  
480 recommendations into future manuscripts, presentations and teaching materials.

481

482

#### **Competing interests**

483

E.G. is founder and CEO of Oroboros Instruments, Innsbruck, Austria. The other authors declare no  
484 competing financial interests.

485

486 **Tables**

487

488

489

490

491

492

**Table 1 | Coupling control states and rates, and residual oxygen consumption in mitochondrial preparations.** Respiration- and phosphorylation-flux,  $J_{\text{kO}_2}$  and  $J_{\text{P}}$ , are rates, characteristic of a state in conjunction with the protonmotive force,  $pmF$ . Coupling states are established at kinetically-saturating concentrations of oxidizable 'fuel' substrates and  $\text{O}_2$ .

State	Rate	$J_{\text{kO}_2}$	$J_{\text{P}}$	$pmF$	Inducing factors	Limiting factors
LEAK	$L$	low, cation leak-dependent respiration	0	max.	back-flux of cations including proton leak, proton slip	$J_{\text{P}} = 0$ : (1) without ADP, $L(n)$ ; (2) max. ATP/ADP ratio, $L(T)$ ; or (3) inhibition of the phosphorylation-pathway, $L(O_{my})$
OXPHOS	$P$	high, ADP-stimulated respiration, OXPHOS-capacity	max.	high	kinetically-saturating [ADP] and $[P_i]$	$J_{\text{P}}$ by phosphorylation-pathway capacity; or $J_{\text{kO}_2}$ by ET-capacity
ET	$E$	max., noncoupled respiration, ET-capacity	0	low	optimal external uncoupler concentration for max. $J_{\text{O}_2, E}$	$J_{\text{kO}_2}$ by ET-capacity
ROX	$R_{ox}$	min., residual $\text{O}_2$ consumption	0	0	$J_{\text{O}_2, R_{ox}}$ in non-ET-pathway oxidation reactions	inhibition of all ET-pathways; or absence of fuel substrates

493

494  
495**Table 2 | Terms on respiratory coupling and uncoupling**

Term	$J_{kO_2}$	$P \gg O_2$	Notes	
intrinsic, no protonophore added	uncoupled	$L$	0	non-phosphorylating <b>LEAK-respiration</b> (Fig. 2)
	proton leak-uncoupled		0	component of $L$ , $H^+$ diffusion across the mtIM (Fig. 2b-d)
	inducibly uncoupled		0	by UCP1 or cation ( <i>e.g.</i> , $Ca^{2+}$ ) cycling; strongly stimulated by permeability transition (mtPT); experimentally induced by valinomycin in the presence of $K^+$
	decoupled		0	component of $L$ , proton slip when protons are effectively not pumped in the redox proton pumps CI, CIII and CIV or are not driving phosphorylation ( $F_1F_0$ -ATPase) <sup>25</sup> (Fig. 2b-d)
	loosely coupled		0	component of $L$ , lower coupling due to superoxide formation and bypass of proton pumps by electron leak with univalent reduction of $O_2$ to superoxide ( $O_2^{\cdot-}$ ; superoxide anion radical)
dyscoupled		0	mitochondrial dysfunction due to pathologically, toxicologically, environmentally increased uncoupling	
noncoupled	$E$		0	ET-capacity, non-phosphorylating respiration stimulated to maximum flux at optimum exogenous protonophore concentration (Fig. 2d)
well-coupled	$P$	high		<b>OXPHOS-capacity</b> , phosphorylating respiration with an intrinsic LEAK component (Fig. 2c)
fully coupled	$P - L$	max.		<b>OXPHOS-capacity</b> corrected for LEAK-respiration (Fig. 2a)
acoupled			0	electron transfer in mitochondrial fragments without vectorial proton translocation upon loss of vesicular (compartmental) integrity

496  
497

498 **Table 3 | Conversion of units**

499 **a. Conversion of O<sub>2</sub> flow,  $I_{O_2}$ , to SI units (International System of Units).**  
 500  $e^-$  is the number of electrons or reducing equivalents)

1 Unit		Multiplication factor	SI-unit
ng.atom O·s <sup>-1</sup>	(2 e <sup>-</sup> )	0.5	nmol O <sub>2</sub> ·s <sup>-1</sup>
ng.atom O·min <sup>-1</sup>	(2 e <sup>-</sup> )	8.333	pmol O <sub>2</sub> ·s <sup>-1</sup>
natom O·min <sup>-1</sup>	(2 e <sup>-</sup> )	8.333	pmol O <sub>2</sub> ·s <sup>-1</sup>
nmol O <sub>2</sub> ·min <sup>-1</sup>	(4 e <sup>-</sup> )	16.67	pmol O <sub>2</sub> ·s <sup>-1</sup>
nmol O <sub>2</sub> ·h <sup>-1</sup>	(4 e <sup>-</sup> )	0.2778	pmol O <sub>2</sub> ·s <sup>-1</sup>

501

502 **b. Conversion of units with preservation of numerical values**  
 503

Name	Frequently used unit	Equivalent unit	Notes
volume-specific flux, $J_{V,O_2}$	pmol·s <sup>-1</sup> ·mL <sup>-1</sup>	nmol·s <sup>-1</sup> ·L <sup>-1</sup>	1
	mmol·s <sup>-1</sup> ·L <sup>-1</sup>	mol·s <sup>-1</sup> ·m <sup>-3</sup>	
cell-specific flow, $I_{O_2/N_{ce}}$	pmol·s <sup>-1</sup> ·10 <sup>-6</sup> cells	amol·s <sup>-1</sup> ·cell <sup>-1</sup>	2
	pmol·s <sup>-1</sup> ·10 <sup>-9</sup> cells	zmol·s <sup>-1</sup> ·cell <sup>-1</sup>	3
cell number concentration, $C_{N_{ce}}$	10 <sup>6</sup> cells·mL <sup>-1</sup>	10 <sup>9</sup> cells·L <sup>-1</sup>	
mitochondrial protein concentration, $C_{mtE}$	0.1 mg·mL <sup>-1</sup>	0.1 g·L <sup>-1</sup>	
mass-specific flux, $J_{O_2/m}$	pmol·s <sup>-1</sup> ·mg <sup>-1</sup>	nmol·s <sup>-1</sup> ·g <sup>-1</sup>	4
volume, $V$	1,000 L	m <sup>3</sup> (1,000 kg)	
	L	dm <sup>3</sup> (kg)	
	mL	cm <sup>3</sup> (g)	
	μL	mm <sup>3</sup> (mg)	
	fL	μm <sup>3</sup> (pg)	
amount of substance concentration	M = mol·L <sup>-1</sup>	mol·dm <sup>-3</sup>	5

504 1 pmol: picomole = 10<sup>-12</sup> mol505 2 amol: attomole = 10<sup>-18</sup> mol506 3 zmol: zeptomole = 10<sup>-21</sup> mol

507

4 nmol: nanomole = 10<sup>-9</sup> mol5 fL: femtoliter = 10<sup>-15</sup> L

**Table 4 | Terms, symbols, and units.** SI base units are used, except for the liter [L = dm<sup>3</sup>]

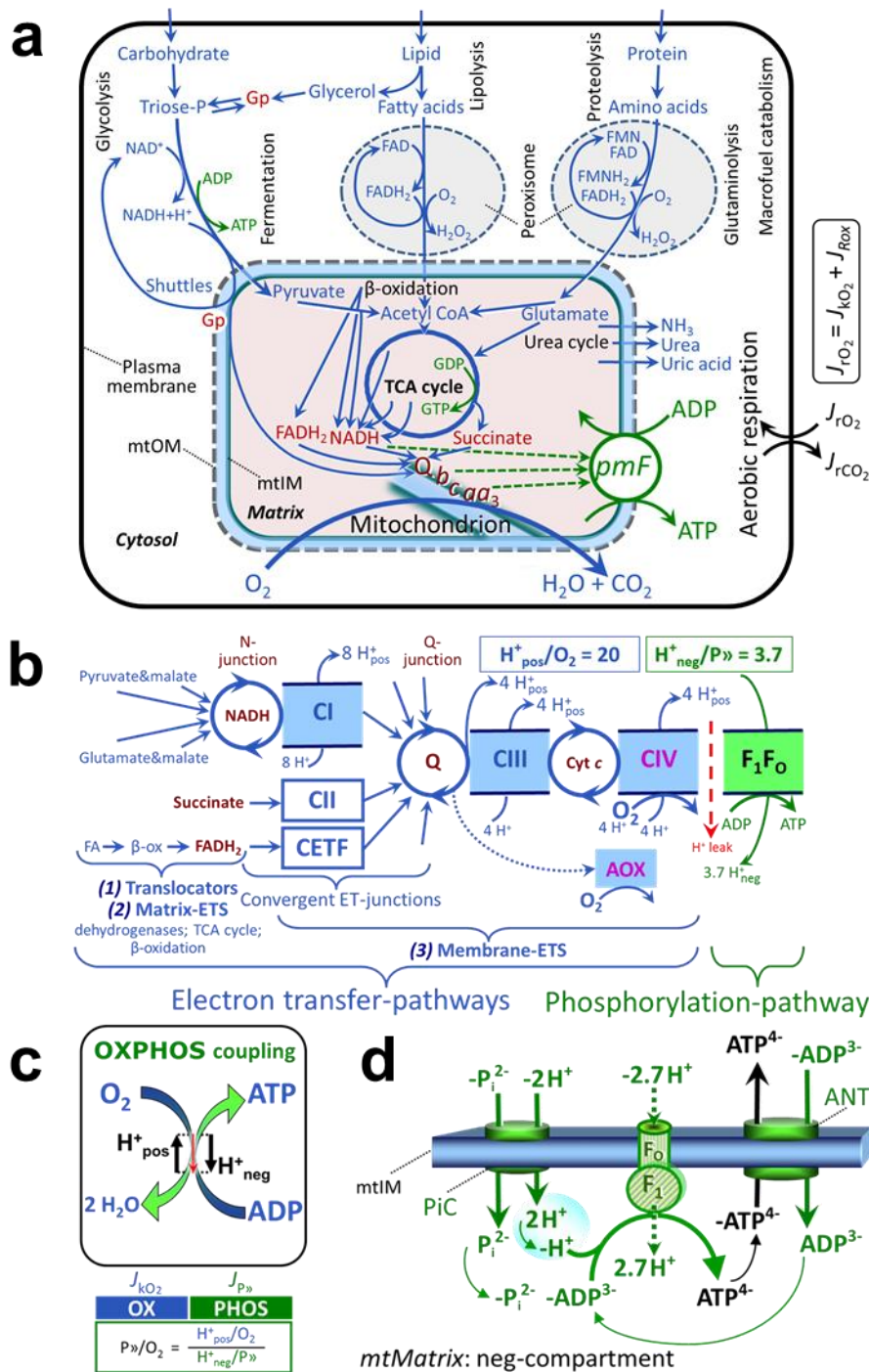
Term	Symbol	Unit	Links and comments
adenosine diphosphate	ADP		Tab. 1; Fig. 1 and 2
adenosine triphosphate	ATP		Tab. 1; Fig. 1 and 2
ATP hydrolysis ATP→ADP	P«		Fig. 2b,c
catabolic reaction	k		Tab. 1 and 2; Fig. 1 and 2
catabolic respiration	$J_{kO_2}$	<i>varies</i>	Fig 1c, Fig. 2b-d
cell concentration (number [x])	$C_{N_{ce}}$	[x·L <sup>-1</sup> ]	for normalization of rate
coenzyme Q-junction	Q-junction		Fig. 1b
electron transfer Complexes	CI to CIV		Fig. 1b; F <sub>1</sub> F <sub>0</sub> -ATPase is not an ET- but a phosphorylation-pathway Complex, hence the term Complex V should not be used
electron transfer, state	ET		Tab. 1; Fig. 2a (State 3u)
electron transfer system	ETS		Fig. 1b
ET-capacity	$E$	<i>varies</i>	Tab. 1; Fig. 2a,d; rate
ET-excess capacity	$E-P$	<i>varies</i>	Fig. 2a
flow	$I$	[mol·s <sup>-1</sup> ]	Fig. 3; extensive quantity
flux	$J$	<i>varies</i>	Fig. 3; size-specific quantity
inorganic phosphate	P <sub>i</sub>		Fig. 1d
inorganic phosphate carrier	PiC		Fig. 1d
LEAK-state	<b>LEAK</b>		Tab. 1; Fig. 2a (compare State 4)
LEAK-respiration	$L$	<i>varies</i>	rate; Tab. 1; Fig. 2a,b
mass of sample or object $X$	$m_X$ or $m_{NX}$	[kg] or [kg·x <sup>-1</sup> ]	Fig. 3
mass, dry mass	$m_d$	[kg] or [kg·x <sup>-1</sup> ]	(dry weight)
mass, wet mass	$m_w$	[kg] or [kg·x <sup>-1</sup> ]	(wet weight)
mitochondria or mitochondrial	mt		compare mtDNA
mitochondrial elementary marker	$mtE$	[mtEU]	Fig. 3; quantity of mt-marker
mitochondrial elementary unit	mtEU	<i>varies</i>	Fig. 3; specific units for mt-marker
mitochondrial inner membrane	mtIM		Fig. 1 (MIM)
mitochondrial outer membrane	mtOM		Fig. 1 (MOM)
NADH-junction	N-junction		Fig. 1b
number concentration of $X$	$C_{NX}$	[x·L <sup>-1</sup> ]	for normalization of rate
number format	$\underline{N}$	[x]	Fig. 3
number of cells	$N_{ce}$	[x]	for normalization of rate
number of entities $X$	$N_X$	[x]	Fig. 3; x is not an SI unit <sup>27</sup>
O <sub>2</sub> concentration	$c_{O_2} = n_{O_2} \cdot V^{-1}$	[mol·L <sup>-1</sup> ]	[O <sub>2</sub> ]
O <sub>2</sub> flow per countable object	$I_{O_2/NX}$	[mol·s <sup>-1</sup> ·x <sup>-1</sup> ]	Fig. 3
O <sub>2</sub> flow per chamber	$I_{O_2}$	[mol·s <sup>-1</sup> ]	Fig. 3
O <sub>2</sub> flux, in reaction r	$J_{rO_2}$	<i>varies</i>	Fig. 1a
O <sub>2</sub> flux, volume-specific	$J_{V,O_2}$	[mol·s <sup>-1</sup> ·L <sup>-1</sup> ]	Fig. 3; per volume of chamber
O <sub>2</sub> flux, sample mass-specific	$J_{O_2/mX}$	[mol·s <sup>-1</sup> ·kg <sup>-1</sup> ]	Fig. 3; specify dry or wet mass
oxidative phosphorylation	OXPHOS		Fig. 1
OXPHOS-state	<b>OXPHOS</b>		Tab. 1; Fig. 2a; OXPHOS-state distinguished from the process OXPHOS (State 3 at kinetically-saturating [ADP] and [P <sub>i</sub> ])
OXPHOS-capacity	$P$	<i>varies</i>	rate; Tab. 1; Fig. 2a,c
permeability transition	mtPT		Tab. 2; MPT is widely used
phosphorylation flux ADP→ATP	$J_{P\gg}$	<i>varies</i>	Fig. 2b-d
phosphorylation of ADP to ATP	P»		Fig. 1
P»/O <sub>2</sub> ratio	P»/O <sub>2</sub>		mechanistic $Y_{P\gg/O_2}$ , calculated from pump stoichiometries; Fig. 1c

565	proton in the negative compartment	$H^+_{neg}$		Fig. 2b-d
566	proton in the positive compartment	$H^+_{pos}$		Fig. 1b,c; Fig. 2b-d
567	protonmotive flux to the negative			
568	compartment	$J_{mH+neg}$	<i>varies</i>	Fig. 2d,f
569	protonmotive flux to the positive			
570	compartment	$J_{mH+pos}$	<i>varies</i>	Fig. 2b,c,d
571	protonmotive force	$pmF$	[V]	Figures 1, 2A and 4; Table 1
572	rate of electron transfer in ET-state	$E$	<i>varies</i>	Tab. 1; ET-capacity
573	rate of LEAK-respiration	$L$	<i>varies</i>	Tab. 1; $L(n)$ , $L(T)$ , $L(O_{my})$
574	rate of oxidative phosphorylation	$P$	<i>varies</i>	Tab. 1; OXPHOS-capacity
575	rate of residual oxygen consumption	$Rox$	<i>varies</i>	Tab. 1
576	residual oxygen consumption, state	ROX		Tab. 1
577	sample type	$X$		
578	tricarboxylic acid cycle	TCA cycle		Fig. 1a
579	volume	$V$	[L]	volume of chamber
580	volume format	$\underline{V}$	[L]	Fig. 3
581	volume of sample or object $X$	$V_X$ or $V_{\underline{X}}$	[L] or $[L \cdot X^{-1}]$	Fig. 3
582				
583				

---

584 **Figures**

585



586

587

588

589

590

591

592

593

594

595

596

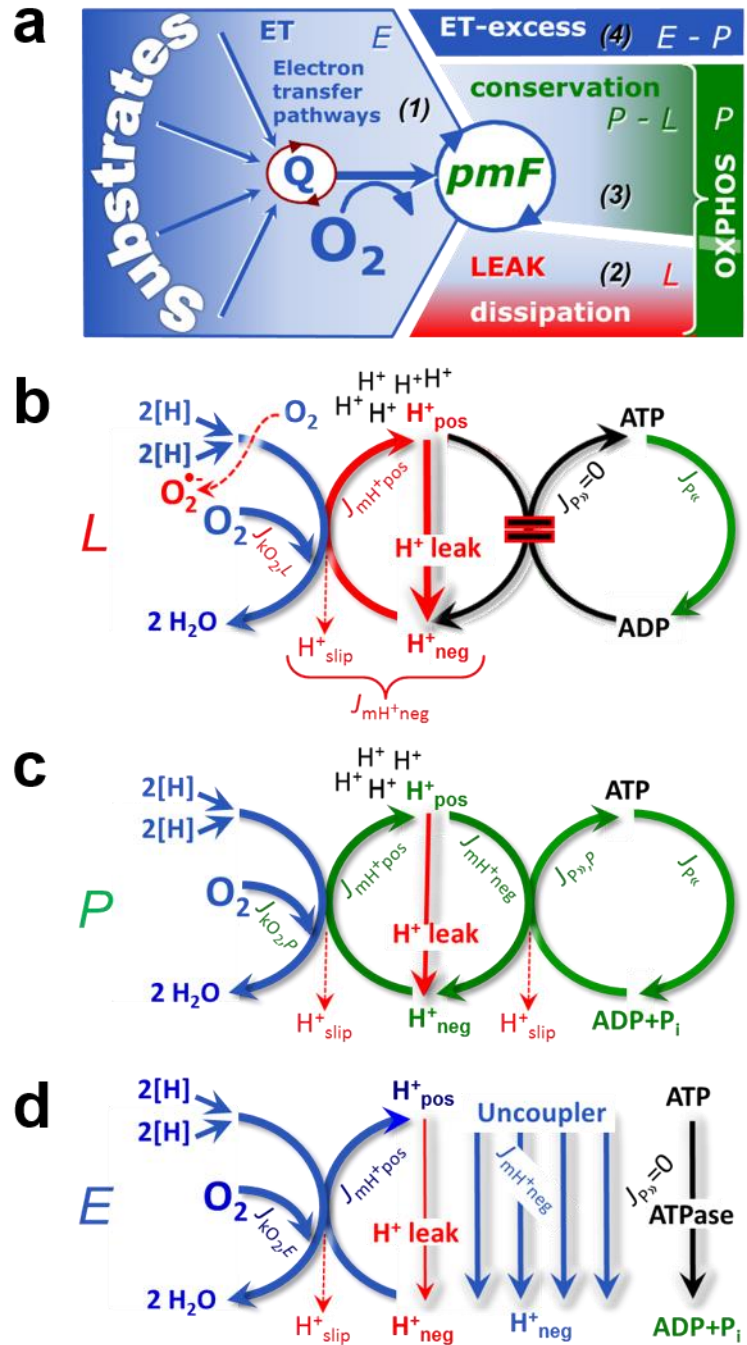
597

**Fig. 1. | Respiration and oxidative phosphorylation (OXPHOS).** (a) Cell respiration: uptake of small molecules and catabolism of macronutrients provide the mitochondrial fuel substrates (electron donors), which are oxidized with electron transfer to  $O_2$  (electron acceptor). Dashed arrows indicate the connection between the redox proton pumps (respiratory Complexes CI, CIII and CIV) and the transmembrane protonmotive force,  $pmF$ . Coenzyme Q (Q) and the cytochromes  $b$ ,  $c$ , and  $aa_3$  are redox systems of the mitochondrial inner membrane, mtIM. Glycerol-3-phosphate, Gp. (b) Mitochondrial respiration: The mitochondrial electron transfer system (ETS) is (1) fueled by diffusion and transport of substrates across the mitochondrial outer and inner membranes (mtOM and mtIM), and in addition consists of the (2) matrix-ETS, and (3) membrane-ETS. Electron transfer converges from dehydrogenases at the NADH-junction (N-junction), and from CI,

598 CII and electron transferring flavoprotein complex (CETF) at the Coenzyme Q-junction  
599 (Q-junction). Unlabeled arrows converging at the Q-junction indicate additional ETS-  
600 sections with electron entry into Q through Gp-dehydrogenase, dihydroorotate  
601 dehydrogenase, proline dehydrogenase, choline dehydrogenase, and sulfide-ubiquinone  
602 oxidoreductase. The dotted arrow indicates the branched pathway of oxygen consumption  
603 by alternative quinol oxidase (AOX). ET-pathways are coupled to the phosphorylation-  
604 pathway. The  $H^+_{\text{pos}}/O_2$  ratio is the outward proton flux from the matrix space to the  
605 positively (pos) charged vesicular compartment, divided by catabolic  $O_2$  flux in the NADH-  
606 pathway<sup>27</sup>. The  $H^+_{\text{neg}}/P_{\gg}$  ratio is the inward proton flux from the inter-membrane space to  
607 the negatively (neg) charged matrix space, divided by phosphorylation flux of ADP to ATP.  
608 These stoichiometries are not fixed because of ion leaks and proton slip. Moreover, the  
609  $H^+_{\text{neg}}/P_{\gg}$  ratio is linked to the  $F_1F_0$ -ATPase *c*-ring stoichiometry, which is species-  
610 dependent and defines the bioenergetic cost of  $P_{\gg}$ . Modified from ref. <sup>28</sup>. **(c)** OXPPOS-  
611 coupling: The  $H^+$  circuit couples  $O_2$  flux through the catabolic ET-pathway,  $J_{\text{KO}_2}$ , to flux  
612 through the phosphorylation-pathway of ADP to ATP,  $J_{P_{\gg}}$ . **(d)** Phosphorylation-pathway:  
613 the proton pump  $F_1F_0$ -ATPase (F-ATPase, ATP synthase), adenine nucleotide translocase  
614 (ANT), and inorganic phosphate carrier (PiC). The  $H^+_{\text{neg}}/P_{\gg}$  stoichiometry is the sum of the  
615 coupling stoichiometry in the F-ATPase reaction ( $-2.7 H^+_{\text{pos}}$  from the positive  
616 intermembrane space,  $2.7 H^+_{\text{neg}}$  to the matrix, *i.e.*, the negative compartment) and the proton  
617 balance in the translocation of  $ADP^{3-}$ ,  $ATP^{4-}$  and  $P_i^{2-}$  (negative for substrates) <sup>12</sup>. Modified  
618 from ref. <sup>8</sup>.  
619



620 **Fig. 2 | Respiratory states and**  
 621 **rates. (a)** Four-compartment model  
 622 of oxidative phosphorylation:  
 623 respiratory states (ET, OXPHOS,  
 624 LEAK) and corresponding rates ( $E$ ,  
 625  $P$ ,  $L$ ) are connected by the  
 626 protonmotive force,  $pmF$ . (1) ET-  
 627 capacity,  $E$ , is partitioned into (2)  
 628 dissipative LEAK-respiration,  $L$ ,  
 629 when the Gibbs energy change of  
 630 catabolic  $O_2$  flux is irreversibly lost,  
 631 (3) net OXPHOS-capacity,  $P-L$ , with  
 632 partial conservation of the capacity  
 633 to perform work, and (4) the ET-  
 634 excess capacity,  $E-P$ . (b) **LEAK-**  
 635 **rate,  $L$** : Oxidation only, since  
 636 phosphorylation is arrested,  $J_{P\gg} = 0$ ,  
 637 and catabolic  $O_2$  flux,  $J_{kO_2,L}$ , is  
 638 controlled mainly by the proton leak  
 639 and slip,  $J_{mH^{+neg}}$  (motive, subscript  
 640 m), at maximum protonmotive force.  
 641 ATP may be hydrolyzed by  
 642 ATPases,  $J_{P\ll}$ ; then phosphorylation  
 643 must be blocked. (c) **OXPHOS-**  
 644 **rate,  $P$** : Oxidation coupled to  
 645 phosphorylation,  $J_{P\gg}$ , which is  
 646 stimulated by kinetically-saturating  
 647 [ADP] and  $[P_i]$ , supported by a high  
 648 protonmotive force maintained by  
 649 pumping of protons to the positive  
 650 compartment,  $J_{mH^{+pos}}$ .  $O_2$  flux,  $J_{kO_2,P}$ ,  
 651 is well-coupled at a  $P\gg/O_2$  flux ratio  
 652 of  $J_{P\gg,P}/J_{O_2,P}$ . Extramitochondrial  
 653 ATPases may recycle ATP,  $J_{P\ll}$ . (d)  
 654 **ET- rate,  $E$** : Oxidation only, since  
 655 phosphorylation is zero,  $J_{P\gg} = 0$ , at  
 656 optimum exogenous uncoupler  
 657 concentration when noncoupled  
 658 respiration,  $J_{kO_2,E}$ , is maximum. The  
 659  $F_1F_0$ -ATPase may hydrolyze ATP  
 660 entering the mitochondria. Modified  
 661 from ref. <sup>8</sup>.  
 662



663 **Fig. 3 | Different meanings of**  
 664 **rate: flow and flux dependent on**  
 665 **normalization for sample or**  
 666 **instrumental chamber.**

667 Fundamental distinction between  
 668 metabolic rate related to the  
 669 experimental sample (left) or to  
 670 the instrumental chamber (right).  
 671 Left: Results are expressed as  
 672 mass-specific *flux*,  $J_{mX}$ , per mg  
 673 protein, dry or wet mass. Cell  
 674 volume,  $V_{ce}$ , may be used for  
 675 normalization (volume-specific  
 676 flux,  $J_{Vce}$ ). Normalization per  
 677 mitochondrial elementary marker,  
 678 *mtE*, relies on determination of mt-  
 679 markers expressed in various  
 680 mitochondrial elementary units [mtEU]. Right: Flow per instrumental chamber,  $I$ , or flux per chamber  
 681 volume,  $J_V$ , are reported for methodological reasons.  
 682

